

# Doping efficiency, dopant location, and oxidation of Si nanocrystals

X. D. Pi,<sup>1,a)</sup> R. Gresback,<sup>1</sup> R. W. Liptak,<sup>2</sup> S. A. Campbell,<sup>2</sup> and U. Kortshagen<sup>1,b)</sup>

<sup>1</sup>Department of Mechanical Engineering, University of Minnesota, Minneapolis, Minnesota 55455, USA

<sup>2</sup>Department of Electrical and Computer Engineering, University of Minnesota, Minneapolis, Minnesota 55455, USA

(Received 13 October 2007; accepted 22 February 2008; published online 25 March 2008)

Gas-phase plasma-synthesized silicon nanocrystals (Si-NCs) are doped with boron (B) or phosphorous (P) during synthesis. The doping efficiency of B is smaller than that of P, consistent with the theoretical prediction of impurity formation energies. Despite vastly different synthesis conditions, the effect of doping on the photoluminescence (PL) of gas-phase-synthesized Si-NCs is qualitatively similar to that of Si-NCs doped during solid phase nucleation. Studies of oxidation-induced changes in PL and etching-induced changes in dopant concentration show that P resides at or near the Si-NC surface, while B is in the Si-NC cores. The oxidation of Si-NCs follows the Cabrera–Mott mechanism [N. Cabrera and N. F. Mott, *Rep. Prog. Phys.* **12**, 163 (1948)].

© 2008 American Institute of Physics. [DOI: 10.1063/1.2897291]

Doping of bulk Si has been critical to the success of the microelectronics industry. This has stimulated similar efforts to dope Si nanocrystals (Si-NCs).<sup>1–9</sup> Fujii *et al.*<sup>1–5</sup> doped Si-NCs embedded in silicon oxide with B or P in the solid phase, where the growth and doping of Si-NCs were typically achieved at temperatures of  $\geq 1100$  °C in 30 min. The authors showed that the photoluminescence (PL) of Si-NCs is attenuated by B doping or high-concentration P doping. They linked the decrease in PL efficiency to the Auger effect. When P was doped at a low concentration, the PL of Si-NCs was usually enhanced. The authors suggested that P passivated defects such as dangling bonds located at the Si-NC/oxide interface. Švrček *et al.*<sup>6</sup> and Tchegotareva *et al.*<sup>7</sup> also observed the similar effect of P doping on the PL of Si-NCs embedded in silicon oxide.

For applications that are targeted at exploiting the modified electrical properties of doped Si-NCs, embedded Si-NCs in a dielectric such as silicon oxide are likely not a good choice, as the matrix prohibits efficient charge transport among Si-NCs. Furthermore, accurately controlling the dopant concentration in embedded Si-NCs is complicated, as dopants may be incorporated in the Si-NCs or reside in the matrix. These problems are absent for freestanding Si-NCs. Baldwin *et al.*<sup>8</sup> synthesized P-doped freestanding Si-NCs in the liquid phase. A P concentration of 6% in Si-NCs was achieved. Impurities associated with the liquid chemical reaction scheme, however, prevented detailed optical characterization of the P-doped Si-NCs. In this letter, we present an investigation on the gas-phase doping of freestanding Si-NCs with at least partial hydrogen coverage of their surface.<sup>10</sup>

The nonthermal plasma system used to synthesize intrinsic and doped Si-NCs was similar to that described in previous work.<sup>11–13</sup> The doping was achieved by introducing dopant precursors (diborane and phosphine) into the plasma. A transmission electron microscope (FEI Tecnai T12) was employed to examine the crystallinity and size of Si-NCs that were deposited on lacy carbon grids. Elemental analysis was carried out via an inductively coupled plasma atomic emission spectrometer (ICP-AES) (Perkin-Elmer Optima

3000DV). For ICP-AES studies, B-doped Si-NCs were dispersed in HNO<sub>3</sub> solution (H<sub>2</sub>O:69% HNO<sub>3</sub>=9:1), while P-doped Si-NCs were dispersed in HCl solution (H<sub>2</sub>O:37% HCl=9:1). All solutions were contained in plastic bottles. The ICP-AES characterizations of B, P, and Si were calibrated by using standard samples. A Spex Fluorolog-2 spectrofluorometer was used to measure PL from Si-NCs that were excited at 325 nm by a Xe lamp. The PL measurements were performed within  $\sim 5$  min after Si-NC production and again after five-day exposure to air at room temperature. All PL spectra were corrected for the spectral system response.

The crystallinity of both intrinsic and doped Si-NCs is evidenced by transmission electron microscopy (TEM) investigations. Statistical analysis on the size  $d$  of Si-NCs gives  $d=3.6 \pm 0.8$  nm. TEM studies show that doping does not affect the nanocrystal size and crystallinity.

Assuming a doping efficiency of 100%, we can calculate the ideal atomic concentrations  $C_i$  of dopants from gas flow rates. Figure 1 compares the actual atomic concentrations  $C_m$  of dopants obtained from ICP-AES measurements with the ideal ones. For P doping,  $C_m$  is almost equal to  $C_i$  when  $C_i$  is smaller than  $\sim 4\%$ , indicating nearly 100% doping efficiencies ( $C_m/C_i$ ) in this range. When  $C_i$  is further increased up to 9%,  $C_m$  is reduced to  $\sim 63\%$  of  $C_i$ . This means that it is less

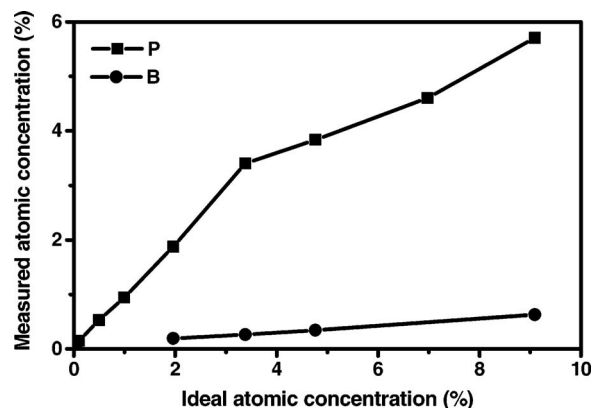


FIG. 1. Dopant atomic concentration measured by ICP-AES vs ideal dopant atomic concentration calculated from the silicon and dopant precursor flow rates. Solid lines are drawn to guide the eyes.

<sup>a)</sup>Electronic mail: xdpi@umn.edu.

<sup>b)</sup>Electronic mail: uk@me.umn.edu.

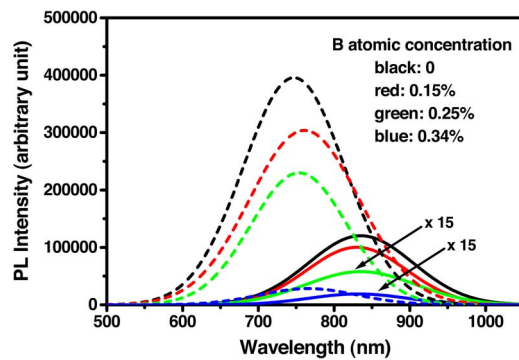


FIG. 2. (Color online) PL spectra from as-synthesized intrinsic and B-doped Si-NCs (solid lines) and the same Si-NCs after five-day exposure to air at room temperature (dashed lines). The B-doped Si-NCs are labeled according to B atomic concentrations obtained from ICP-AES measurements. The intensity of PL from as-synthesized Si-NCs with B concentrations of 0.25% and 0.34% is magnified by a factor of 15.

efficient to dope Si-NCs with P at high concentrations. For B doping,  $C_m$  is much smaller than  $C_i$ ; the doping efficiency of B is approximately ten times smaller than that of P. Recent computational studies demonstrated that in Si-NCs the formation energy of substitutional B is larger than that of substitutional P when structure relaxation after doping is not involved.<sup>14</sup> Our observation that B is less efficiently doped than P appears to support this theoretical prediction.

Figure 2 shows the PL spectra from as-synthesized intrinsic and B-doped Si-NCs and from the same Si-NCs exposed to air at room temperature for 5 days. The PL intensity ( $I_{PL}$ ) of as-synthesized Si-NCs decreases with increasing B concentration. As discussed in Refs. 1 and 2, this suggests that B in Si-NCs is ionized, giving rise to Auger recombination, which quenches the light emission from Si-NCs. Furthermore, a B atom is  $\sim 21\%$  smaller than a Si atom, causing considerable strain in B-doped Si.<sup>14–16</sup> Strain-induced defect states may further quench the light emission from Si-NCs. We observe that with an increase of B concentration up to 0.34%,  $I_{PL}$  decreases by a factor up to  $\sim 100$ . At very small doping levels of  $<0.05\%$  (not shown), the PL of Si-NCs remains unaffected. Figure 2 shows that after 5 days of exposure to air, the PL from both intrinsic and B-doped Si-NCs blueshifts. This effect is attributed to the oxidation-induced reduction of Si-NC size.<sup>10,13,16</sup> It was suggested that Si-NC/oxide interface is less defective than the surface of as-synthesized Si-NCs.<sup>13</sup> This explains the increase in  $I_{PL}$  for all Si-NCs after oxidation. However, despite the overall increase in  $I_{PL}$ , the B-doped Si-NCs still emit light less efficiently than intrinsic Si-NCs. This indicates that B dopants remain active in spite of the formation of oxide shells around SiNCs, which implies that B dopants are incorporated in the Si-NC cores.

The PL spectra from as-synthesized intrinsic and P-doped Si-NCs and from the same Si-NCs exposed to air at room temperature for 5 days are shown in Fig. 3. Different from B doping,  $I_{PL}$  of P-doped Si-NCs is larger than that of intrinsic Si-NCs at small dopant concentrations, such as 0.06%. As nonradiative states that reduce  $I_{PL}$  are believed to be located at the Si-NC surface, this increase in  $I_{PL}$  suggests that P dopants reside at the surface and passivate some of these nonradiative surface states such as dangling bonds, as proposed in Refs. [3,4]. This hypothesis is corroborated by the fact that the segregation coefficient  $\kappa$ , which is the ratio

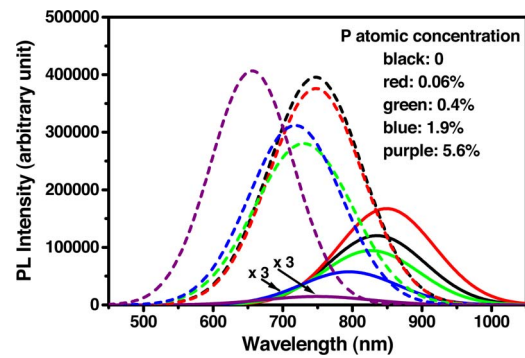


FIG. 3. (Color online) PL spectra from as-synthesized intrinsic and P-doped Si-NCs (solid lines) and the same Si-NCs after five-day exposure to air at room temperature (dashed lines). The P-doped Si-NCs are labeled according to P atomic concentrations obtained from ICP-AES measurements. The intensity of PL from as-synthesized Si-NCs with P concentrations of 1.9% and 5.6% is magnified by a factor of 3.

of dopant concentration at the surface to that in the core during epitaxial growth, is much larger for P than for B,<sup>17</sup> suggesting that P has a much stronger tendency to stay at Si-NC surface than B. At a given  $\kappa$ , the number of P atoms embedded into Si-NCs increases with increasing P concentration, finally leading to the activation of P dopants by ionization. The free electrons then lead to Auger recombination<sup>4,5</sup> (in contrast to B, strain-induced defect states may be negligible because the atomic size difference between P and Si is small). Therefore,  $I_{PL}$  of P-doped Si-NCs becomes smaller than that of intrinsic Si-NCs when the concentration of P exceeds 0.4%. Similar to B doping, the PL is attenuated more significantly with the further increase of P concentration up to 5.6%. The preferential doping of larger Si-NCs in an ensemble<sup>7</sup> may lead to the blueshift of PL at high P concentrations. At low concentrations for P and B, the effect of preferential doping should be less pronounced and, hence, the peak position of the PL is nearly unaffected.

Interestingly, after 5 days of exposure to air,  $I_{PL}$  of all P-doped Si-NCs becomes comparable to that of intrinsic Si-NCs, implying that P-induced modification of  $I_{PL}$  has ceased as a result of oxidation. This further indicates that P dopants are located at or near the surface. After surface oxidation, the P dopants appear to become embedded in silicon oxide no longer exhibiting an effect on the PL from Si-NCs.

To independently probe the locations of dopants, the surface oxide layer of Si-NCs, formed after 5 days of oxidation in air, was removed by  $\sim 1$  wt. % HF etching. After the etching, Si-NCs were collected on polyvinylidene fluoride membrane filters (0.1  $\mu\text{m}$  pore size, Millipore Inc.) and washed with de-ionized water. The etching-induced changes of dopant concentration are shown in Fig. 4. Clearly, P concentration is reduced by  $\sim 80\%$  after etching the surface oxide layer. This corroborates that P is primarily located in the near-surface layer of Si-NCs, which is transformed into silicon oxide during oxidation and removed during etching. Contrarily, B concentration increases after etching when the doping level of B is low. This indicates that B is, indeed, primarily incorporated into the Si-NC cores. The surface oxide layer removed during etching hardly contains B, leading to negligible loss of B in contrast to loss of Si. The etching-induced increase in B concentration declines with increasing B concentration, implying that the distribution of B extends

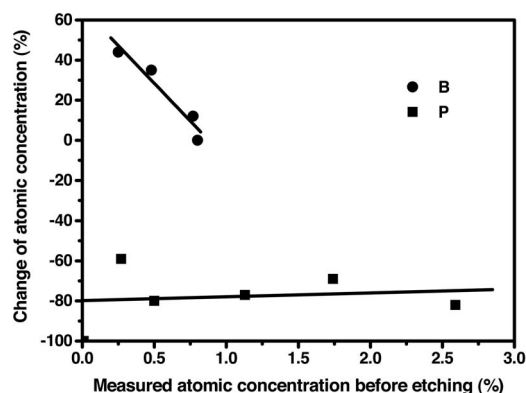


FIG. 4. Change of dopant concentration after the HF etching of Si-NCs that have been exposed to air for 5 days. Solid lines result from linear fits to the data.

from the core toward the surface as the doping level of B increases.

The fact that the modification of PL from Si-NCs with P or B doping for our gas-phase-synthesized Si-NCs is qualitatively similar to that found for solid-phase nucleated Si-NCs (Refs. 1–5) is in itself an interesting finding and quite surprising, since the Si-NC growth and doping conditions in the plasma and in the solid phase are vastly different. In our gas-phase plasma approach, the growth and doping of Si-NCs are realized at a temperature of  $<600^\circ\text{C}$  in a time on the order of a few milliseconds.<sup>11</sup> The solid-phase growth and doping of Si-NCs are typically achieved at temperatures of  $\geq 1100^\circ\text{C}$  in 30 min. As was recently discussed in Ref. 18, different mechanisms are expected to govern the dopant incorporation in different temperature regimes: the incorporation of impurities into nanocrystals is determined by kinetics at low temperature and by thermodynamic equilibrium solubility at high temperature.

It is also interesting to note that the oxidation-induced PL blueshift for Si-NCs with P concentrations of  $\geq 0.4\%$  is more significant than that for intrinsic Si-NCs (Fig. 3). This can be interpreted within the framework of Cabrera–Mott mechanism<sup>19</sup> for the oxidation of Si-NCs at room temperature. For intrinsic Si-NCs, after initial oxidation, electrons tunnel through the silicon oxide shell to reach the surface, inducing an electric field  $E_{\text{ox}}$  that points toward the surface. Oxygen adsorbed at the surface is ionized to become negatively charged. Oxygen ions then diffuse through silicon oxide to oxidize the underlying Si-NC with the assistance of the built-in  $E_{\text{ox}}$  across the silicon oxide. For P-doped Si-NCs, the tunneling of P-induced free electrons, whose concentration is much larger than that of intrinsic electrons, enhances  $E_{\text{ox}}$ . Thus, oxygen ions more quickly travel through the oxide, inducing more efficient oxidation. In contrast to P doping, B doping weakens  $E_{\text{ox}}$ . Therefore, B-doped Si-NCs oxidize more slowly than intrinsic Si-NCs, as evidenced by the fact that the oxidation-induced blueshift for B-doped Si-NCs is less significant than that for intrinsic Si-NCs (Fig. 2).

Finally, we should note that the Si-NCs studied here contain on the order of  $10^3$  atoms. Hence, the number of dopants in a Si-NC is  $>1$  on average for dopant concentrations exceeding  $\sim 0.1\%$ . If every Si-NC is doped and all dopants are ionized, the PL of Si-NCs should be completely quenched by the Auger effect at high dopant concentrations, which is clearly not the case. There may be two mechanisms for the PL to prevail at high dopant concentrations. First, the number of dopants per Si-NC is expected to be statistically distributed, with a small fraction of Si-NCs containing no dopants even if the average number of dopants per Si-NC strongly exceeds one. Second, computational studies<sup>14</sup> found that the activation energy of B and P in 3.6 nm Si-NCs is significantly larger ( $\sim 0.5$  eV) than in bulk Si material. This suggests that only a small fraction of dopants are ionized to generate free carriers at room temperature.

In summary, we have doped freestanding Si-NCs with B or P by a gas-phase plasma approach. The doping efficiency of P is larger than that of B. It is found that B is incorporated into the Si-NC cores, while P resides at or near the Si-NC surface. The oxidation kinetics of Si-NCs is consistent with the Cabrera–Mott mechanism.

The authors are grateful to Professor David J. Norris for support in the PL measurements. Russell Anderson is thanked for the ICP-AES measurements. This work was supported primarily by the MRSEC Program of the NSF under Award No. DMR-0212302, and partially by NSF Grant No. DMI-0556163 and IGERT Grant DGE-0114372. Portions of this work were supported through the NSF NNIN Program.

<sup>1</sup>S. H. Y. Kanzawa, M. Fujii, and K. Yamamoto, *Solid State Commun.* **100**, 227 (1996).

<sup>2</sup>M. Fujii, S. Hayashi, and K. Yamamoto, *J. Appl. Phys.* **83**, 7953 (1998).

<sup>3</sup>S. H. M. Fujii, A. Mimura, and K. Yamamoto, *Appl. Phys. Lett.* **75**, 184 (1999).

<sup>4</sup>A. Mimura, M. Fujii, S. Hayashi, D. Kovalev, and F. Koch, *Phys. Rev. B* **62**, 12625 (2000).

<sup>5</sup>M. Fujii, A. Mimura, and S. Hayashi, *Phys. Rev. Lett.* **89**, 206805 (2002).

<sup>6</sup>V. Švrček, A. Slaoui, J.-C. Muller, J.-L. Rehspringer, B. Honerlage, R. Tomasunas, and I. Pelant, *Physica E (Amsterdam)* **16**, 420 (2003).

<sup>7</sup>A. L. Tchegotareva, M. J. A. de Dooda, J. S. Biteen, H. A. Atwater, and A. Polman, *J. Lumin.* **114**, 137 (2005).

<sup>8</sup>R. K. Baldwin, J. Zou, K. A. Pettigrew, G. J. Yeagle, R. D. Britt, and S. M. Kauzlarich, *Chem. Commun. (Cambridge)* **2006**, 658.

<sup>9</sup>R. Lechner, H. Wiggers, A. Ebbes, J. Steiger, M. S. Brandt, and M. Stutzmann, *Phys. Status Solidi (RRL)* **1**, 262 (2007).

<sup>10</sup>X. D. Pi, L. Mangolini, S. A. Campbell, and U. Kortshagen, *Phys. Rev. B* **75**, 085423 (2007).

<sup>11</sup>L. Mangolini, E. Thimsen, and U. Kortshagen, *Nano Lett.* **5**, 655 (2005).

<sup>12</sup>L. Mangolini and U. Kortshagen, *Adv. Mater. (Weinheim, Ger.)* **19**, 2513 (2007).

<sup>13</sup>X. D. Pi, R. W. Liptak, S. A. Campbell, and U. Kortshagen, *Appl. Phys. Lett.* **91**, 083112 (2007).

<sup>14</sup>G. Cantele, E. Degoli, E. Luppi, R. Magri, D. N. Ninno, G. Iadonisi, and S. Ossicini, *Phys. Rev. B* **72**, 113303 (2005).

<sup>15</sup>P. Rai-Choudhury and F. I. Salkovitz, *J. Cryst. Growth* **7**, 361 (1970).

<sup>16</sup>G. Ledoux, O. Guillois, D. Portrat, C. Reynaud, F. Huisken, B. Kohn, and V. Paillard, *Phys. Rev. B* **62**, 15942 (2000).

<sup>17</sup>J. F. Nutzel and G. Abstreiter, *Phys. Rev. B* **53**, 13551 (1996).

<sup>18</sup>D. J. Norris, A. L. Efros, and S. C. Erwin, *Science* (in press).

<sup>19</sup>N. Cabrera and N. F. Mott, *Rep. Prog. Phys.* **12**, 163 (1948).